Available online at www.sciencedirect.com
ScienceDirect
Publishing Services by Elsevier
International Journal of Naval Architecture and Ocean Engineering xx (2016) 1–10
http://www.journals.elsevier.com/international-journal-of-naval-architecture-and-ocean-engineering/

Peridynamic simulation of brittle-ice crushed by a vertical structure

Minghao Liu, Qing Wang*, Wei Lu

College of Ship Engineering, Harbin Engineering University, Harbin 150001, China

Received 25 June 2016; revised 4 September 2016; accepted 18 October 2016
Available online ■ ■ ■

Abstract

Sea ice is the main factor affecting the safety of the Arctic engineering. However, traditional numerical methods derived from classical continuum mechanics have difficulties in resolving discontinuous problems like ice damage. In this paper, a non-local, meshfree numerical method called "peridynamics", which is based on integral form, was applied to simulate the interaction between level ice and a cylindrical, vertical, rigid structure at different velocities. Ice in the simulation was freshwater ice and simplified as elastic-brittle material with a linear elastic constitutive model and critical equivalent strain criterion for material failure in state-based peridynamics. The ice forces obtained from peridynamic simulation are in the same order as experimental data. Numerical visualization shows advantages of applying peridynamics on ice damage. To study the repetitive nature of ice force, damage zone lengths of crushing failure were computed and conclude that damage zone lengths are 0.15–0.2 times as ice thickness.

Keywords: Numerical simulation; Ice–structure interaction; State-based peridynamics; Ice crushing; Ice forces

1. Introduction

With increasing interest in oil and gas exploration in cold regions, human activities in these areas are increasing. In Arctic region, the presence of sea ice is an important factor that contributes to the performance of naval architecture. For this reason, much research has focused on cold-region engineering. Vertical structure is a typical structural form in Arctic ocean engineering, such as the jacket platforms being widely used in Bohai Sea. Ice induced force during interaction of ice and vertical structures attracts great attention from scholars.

Sodhi and Morris (1984) conducted small-scale experiments to measure varied ice forces by pushing rigid cylindrical structures of different diameters at different velocities through a level ice sheet. The small-scale experiments showed that the characteristic frequency maintains a linear relationship with the ratio of velocity to thickness. Scale-model tests of interactions between level ice and conical structures were conducted by Tian and Huang (2012) to verify the lower ice force on the structure, and the experimental flexural strength results were discussed. From 2004 to 2005, Huang et al. (2007) conducted series of model tests to explore the mechanism that controls the procedure of ice induced vibration of vertical narrow piles and setup interaction coefficient that is able to reflect the interaction level of ice and structure. Yue et al. (2009) conducted full-scale tests of interaction between level ice and vertical compliant structures to study dynamic ice forces and structure vibrations. Regarding with loading rate, ductile, ductile–brittle transition and brittle ice failure were observed.

Ice damage during ice–structure interaction is a complex process of material failure. Numerical techniques for addressing discontinuities are of significant interest to researchers. But currently, it is short of a numerical method to simulate the complex failure process of ice (Bergan et al., 2010). For the macro approach based on continuum mechanics, the solution of governing equation is related to the partial derivatives of its stress and relative displacement. However, the numerical methods derived from classical

* Corresponding author.
E-mail address: wangqing@hrbeu.edu.cn (Q. Wang).

http://dx.doi.org/10.1016/j.ijnaoe.2016.10.003

continuum mechanics, which has difficulties in resolving discontinuity, have also restricted the research progress of the polar ocean engineering. Peridynamics is a meshless method to solve the equation of motion by using integral form. Therefore, it has obvious advantages for the simulation of complex material damage.

Silling (2000) proposed the original peridynamic theory called *bond-based peridynamics* in 2000, and it reformulates the continuum mechanics equations. Similar to molecular dynamics, peridynamic equation of motion uses a nonlocal method to describe the force between particles, so that there is no requirement to know the crack location in advance. The essence of the equations is that integration rather than differentiation used in the calculation, which also avoids redefining the body of discontinuity (see Fig. 1). Brbaru et al. (2009) developed adaptive refinement algorithms for non-local peridynamics in elastic material regarding with one dimension model. In addition, compared with classical elasticity, they discussed many types of numerical convergence for peridynamics and obtained uniform convergence to the classical solutions of static and dynamic problems in one dimension in the limit of the horizon going to zero.

Even though bond-based peridynamics shows remarkable ability to deal with discontinuities in material like crack propagation, fracture and damage, its weak relationship with classical mechanics restricts its application on complicated material. As a result, Silling et al. (2007) proposed a more general form of peridynamics, called *state-based peridynamics*, which can adopt the constitutive model directly and reinforce the relationship between peridynamics and classical mechanics. Warren et al. (2009) applied state-based peridynamics to solve deformation and fracture problems in solid materials. Foster et al. (2010) proposed a method to implement a rate-dependent viscoplastic material within this peridynamic model.

The peridynamic theory overcomes weaknesses of existing methods and can simultaneously and spontaneously simulate all failure modes without simplifying assumptions. The efficiency and convenience of this numerical method facilitate its application in deformation and discontinuities of materials.

In this paper, we applied state-based peridynamics, which is a nonlocal theory that uses integration rather than differentiation to calculate material deformation and requires no need for a predefined crack propagation path, to simulate the interaction between level ice and a cylindrical, vertical, rigid structure at different velocities. The basic theory of state-based peridynamics and numerical methods as implemented in the simulation, such as discretization and time-integration stability, were introduced briefly. To implement a two-body interaction in the peridynamic model, an interaction force density in terms of relative positions in the current configuration was applied to prevent material particles that belong to different bodies from sharing the same position. To verify the feasibility and accuracy of applying the peridynamic method to ice–structure interactions, the peridynamic simulation results were compared with small-scale experiments. The results from numerical simulation, including the ice force values, repetitive nature of ice forces, phenomenon of damaged ice, damage zone length and characteristics of ice loading cycle were presented and analyzed.

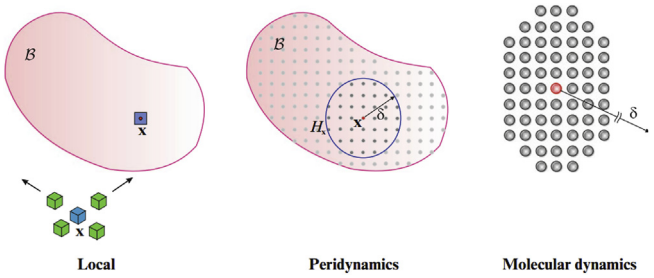

Fig. 1. Comparison of local method, peridynamics and molecular dynamics.

2. Theory of peridynamics

The peridynamic theory divides continuum into discrete material points, see Fig. 3. Therefore, the deformation of body can be described by displacements of points. Each material point interacts with its neighbors by nonlocal forces, see Fig. 2. Integrating the forces acting on a material point leads to its acceleration and velocity with help of Newton's law and avoids the mathematical problems faced in partial differential methods when addressing discontinuities (Silling, 2000). Furthermore, when the relative displacement of material points reaches a critical value, nonlocal force vanishes. This process means appearance of material failure. Additional criteria are not required for determining crack growth and branching, which allows crack growth and branching to proceed spontaneously.

Peridynamics introduces a “horizon” for each material point, in which the material points interact with each other by

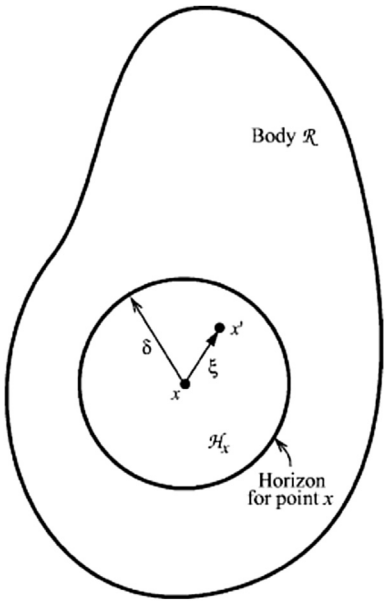

Fig. 2. Each point x in the body interacts with points in its horizon, δ is radius of horizon.

Please cite this article in press as: Liu, M., et al., Peridynamic simulation of brittle-ice crushed by a vertical structure, International Journal of Naval Architecture and Ocean Engineering (2016), http://dx.doi.org/10.1016/j.ijnaoe.2016.10.003

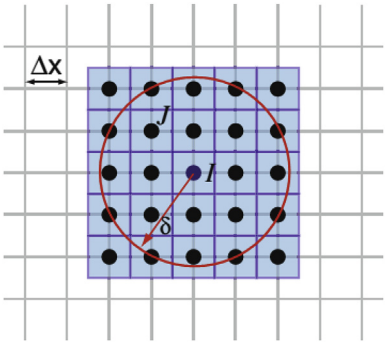

Fig. 3. Configuration of continuum discrete in peridynamics.

"bonds" and forces are integrated over the horizon. As a result, a material point is subjected to forces from not only the nearest points but all points in the horizon, see Fig. 2. It is for this reason that peridynamics is known as a nonlocal method. The points in the horizon of point x are called family points of point x.

The original peridynamic theory, called *bond-based peridynamics*, is a convenient and efficient numerical method to deal with discontinuous problems. However, this original bond-based peridynamics is an oversimplification with the assumption that any pair of material particles interacts with each other only through a central force potential without dependence on other local conditions (Foster et al., 2010). This leads to some critical shortcomings, such as an effective Poisson's ratio of 1/4 and a limited relationship with conventional mechanics. To address these issues, a more general theory termed *state-based peridynamics* was proposed by Silling et al. (2007) and be achieved using the idea of *peridynamic states*. This theory reinforces the relations between peridynamics and classical mechanics and offers an effective method to adopt constitutive models.

We now review the fundamental theory of state-based peridynamic theory briefly. In state-based peridynamics, deformation state $\mathbf{Y}$ and force state $\mathbf{T}$ vectors are defined to associate a vector with each bond $\boldsymbol{\xi} = x - \mathbf{x}'$ within a neighborhood of any point $\mathbf{x}$. The bond that the vector state operates on is written in angle brackets. For state-based peridynamics, the equation of motion can be written as

$$\rho\ddot{\mathbf{u}}[\mathbf{x},t] = \int_{H_x} \{\mathbf{T}[\mathbf{x},t]\langle\mathbf{x}'-\mathbf{x}\rangle - \mathbf{T}[\mathbf{x}',t]\langle\mathbf{x}-\mathbf{x}'\rangle\} dV_{\mathbf{x}'} + \mathbf{b}[\mathbf{x},t] \tag{1}$$

where $\mathbf{T}[\mathbf{x},t]$ is the force-vector state that represents the relationship (bond force) between material points at time t, and maps the deformation-vector state into a force-vector state for each material point. H_x is the space of material points that neighbor point $\mathbf{x}$, which means the area of horizon. ρ is the material density and $\mathbf{b}[\mathbf{x},t]$ is the body force that acts on point $\mathbf{x}$. For convenience, in the following discussion, we denote $\boldsymbol{\xi} = x - \mathbf{x}'$ as the relative position of two points in reference configuration and $\boldsymbol{\eta} = \mathbf{u}[\mathbf{x}',t] - \mathbf{u}[\mathbf{x},t]$ as their relative displacement, where $\mathbf{u}[\mathbf{x},t]$ and $\mathbf{u}[\mathbf{x}',t]$ are displacements of points initially at $\mathbf{x}$ and $\mathbf{x}'$, respectively. The deformation-vector state is defined as

$$\mathbf{Y}[\mathbf{x},t]\langle\boldsymbol{\xi}\rangle = \boldsymbol{\xi} + \boldsymbol{\eta} \tag{2}$$

To associate peridynamics with classical mechanics and to introduce a constitutive model into the theory, a non-local shape tensor for a point $\mathbf{x}$ is defined as

$$\mathbf{K}[\mathbf{x},t] = \int_{H_x} \omega(|\boldsymbol{\xi}|)(\boldsymbol{\xi}\otimes\boldsymbol{\xi}) dV_{\mathbf{x}'} \tag{3}$$

where $\otimes$ is the dyadic product operator and ω is an scalar influence function that is dependent on $|\boldsymbol{\xi}|$. Influence function ω is a parameter whose value is $0 \le \omega \le 1$ and describes the effect degree between a pair of material points. Traditionally, the nearer the two points are, ω is closer to 1. The value of parameter ω needs more investigation. In this paper, we only make ω equal to 0 or 1 and $\omega = 0$ means bond breakage.

With the shape tensor, the non-local deformation gradient $\mathbf{F}$ is given by

$$\mathbf{F}[\mathbf{x},t] = \left[\int_{H_x} \omega(|\boldsymbol{\xi}|)(\mathbf{Y}\langle\boldsymbol{\xi}\rangle\otimes\boldsymbol{\xi}) dV_{\mathbf{x}'}\right]\mathbf{K}^{-1} \tag{4}$$

where $H_x = \{|\mathbf{x}' - \mathbf{x}| < \delta\}$.

To associate force state with material deformation, traditional stress-strain model from classical mechanic theory can be used as an intermediate step. After that, Cauchy stress tensor can be described as a function of deformation gradient, $\boldsymbol{\sigma}(\mathbf{F})$. We can now convert Cauchy stress into first Piola–Kirchhoff stress tensor

$$\mathbf{P} = \det(\mathbf{F})\boldsymbol{\sigma}\mathbf{F}^{-T} \tag{5}$$

The force-vector state can be written as

$$\mathbf{T}\langle\boldsymbol{\xi}\rangle = \omega(|\boldsymbol{\xi}|)\mathbf{P}(\mathbf{F})\mathbf{K}^{-1}\boldsymbol{\xi} \tag{6}$$

where $\mathbf{P}(\mathbf{F})$ is the first Piola-Kirchhoff stress tensor obtained from the constitutive model as a function of deformation gradient. The force state vector can be substituted back into Eq. (1) and to find accelerations at this step. The process of integration is purely meshless Lagrangian at each material point without need for Gauss integration points and interpolation of nodal value.

3. Constitutive model and failure criterion

Ice is a complicated material that is composed of solid ice, brine, gas and depends on temperature, various types of solid salts. Environmentally controlled variations in the mechanisms of ice growth can result in several different grain structures, depending on the prevailing conditions. The most common grain structures are granular, columnar and discontinuous columnar. Granular ice is usually isotropic (ice properties do not depend on the direction of measurement). Furthermore, granular ice can be produced conveniently in indoor

Please cite this article in press as: Liu, M., et al., Peridynamic simulation of brittle-ice crushed by a vertical structure, International Journal of Naval Architecture and Ocean Engineering (2016), http://dx.doi.org/10.1016/j.ijnaoe.2016.10.003

laboratories. Thus, granular ice is a frequently used material in laboratory tests and numerical simulations.

Furthermore, since stress state during ice crushing is mostly compressive, ductile–brittle transition of ice compressive strength should be a complex factor (Jones, 1982). According to Yue et al. (2009), during ice crushing, ice forces represent three modes regarding with loading rate.

(1) When loading rate is lower than 20 mm/s, ice force is quasi-static. Ice is ductile material with plastic mechanical behavior.
(2) When loading rate is between 20 mm/s to 40 mm/s, ice force is defined as locked-in ice force. Ice behaves ductile–brittle transition.
(3) When loading rate is higher than 40 mm/s, ice force becomes irregular. At this state, ice is elastic brittle material.

Several researchers have conducted laboratory tests to examine brittle strength, failure patterns and characteristics of ice–structure interactions (Kuehn et al., 1993; Kamio et al., 2003; Schulson, 1997, 2001; Jordaan, 2001). In addition, the moving velocities of vertical structure in present simulation are higher than 50 mm/s, which means the ice surrounding the structure, behaves mainly elastic brittle ice. Since brittle ice failure plays a critical role in ice failure modes surrounding naval structures, a linear elastic constitutive model is used in this paper with a critical equivalent strain criterion to describe elastic brittle ice.

As described in Section 2, with non-local deformation gradient $\mathbf{F}$, strain of a material point can be obtained. The strain measurement from simulation was calculated by using Green strain as shown in the following equation

$$\mathbf{E} = \frac{1}{2}(\mathbf{F}^T\mathbf{F} - \mathbf{I}) \tag{7}$$

where $\mathbf{I}$ is unit tensor.

For elastic brittle ice in simulation, constitutive model can be numerically updated as

$$\boldsymbol{\sigma} = \mathbf{C} : \mathbf{E} \tag{8}$$

where $\mathbf{C}$ is elastic material tensor.

In peridynamics, various methods exist to determine criteria of material damage. We use a critical equivalent strain to determine breakage of the bond between $\mathbf{x}$ and $\mathbf{x}'$ in elastic brittle freshwater ice in which shear strain plays an important role in material failure. Firstly, we average the values of strains at $\mathbf{x}$ and $\mathbf{x}'$ as $\mathbf{E}(\mathbf{x},\mathbf{x}') = (\mathbf{E}(\mathbf{x}) + \mathbf{E}(\mathbf{x}'))/2$. The equivalent strain can be expressed as

$$E_{eq}(\mathbf{x},\mathbf{x}') = \sqrt{\frac{3}{2}\mathbf{E}_{IJ}(\mathbf{x},\mathbf{x}') : \mathbf{E}_{IJ}(\mathbf{x},\mathbf{x}')} \tag{9}$$

where $\mathbf{E}_{IJ}$ is the deviatoric part of the averaged strain.

If the value of the equivalent strain becomes greater than a critical value, the bond breaks irreversibly. This is similar to critical stretch used in bond-based peridynamics (Silling, 2000), which is a typical method to describe failure in brittle materials.

4. Numerical methods

Peridynamics is typical meshfree numerical method to simulate material fracture. In this section, several numerical methods, including discretization of equation of motion, time integration and numerical stability, are presented for implementation of peridynamics.

4.1. Discretization

After the continuum domain has been discretized by unit cell volumes occupied by material points, Eq. (1) can be transformed to the discretized form

$$\rho(\mathbf{x}_i)\ddot{\mathbf{u}}(\mathbf{x}_i,t) = \sum_{n=1}^{m}\{\mathbf{T}[\mathbf{x}_i,t]\langle\mathbf{x}_n-\mathbf{x}_i\rangle - \mathbf{T}[\mathbf{x}_n,t]\langle\mathbf{x}_i-\mathbf{x}_n\rangle\}V_n + \mathbf{b}(\mathbf{x}_i,t) \tag{10}$$

where $\mathbf{T}$ is the force state function, point i is the subjective point in a given horizon and n is family point in horizon. m is the number of points that interact with point i by unbroken bonds. The unit volume is $V_n = (\Delta x)^3$ for a three-dimensional model and $V_n = (\Delta x)^2$ for a two-dimensional model (Δx is the point spacing).

Similarly, the shape tensor and deformation gradient can be discretized as

$$\mathbf{K}(\mathbf{x}_i) = \sum_{n=1}^{m}\omega(|\mathbf{x}_n-\mathbf{x}_i|)((\mathbf{x}_n-\mathbf{x}_i)\otimes(\mathbf{x}_n-\mathbf{x}_i))V_n \tag{11}$$

and

$$\mathbf{F}(\mathbf{x}_i) = \left[\sum_{n=1}^{m}\omega(|\mathbf{x}_n-\mathbf{x}_i|)(\mathbf{Y}\langle\mathbf{x}_n-\mathbf{x}_i\rangle\otimes(\mathbf{x}_n-\mathbf{x}_i))V_n\right]\mathbf{K}^{-1} \tag{12}$$

4.2. Time integration and numerical stability

To acquire displacements of points, an explicit method is applied to the preceding time integration. According to Eq. (1), acceleration of point i at time step n can be calculated by

$$\ddot{\mathbf{u}}_i^n = \frac{\boldsymbol{f}_i^n + \boldsymbol{b}_i^n}{\rho_i} \tag{13}$$

where $\boldsymbol{f}$ is integral non-local force vector exerting on point i. After accelerations of material points is acquired, explicit algorithm can be used to calculate the velocities and displacements at time t

Please cite this article in press as: Liu, M., et al., Peridynamic simulation of brittle-ice crushed by a vertical structure, International Journal of Naval Architecture and Ocean Engineering (2016), http://dx.doi.org/10.1016/j.ijnaoe.2016.10.003

$$\dot{\mathbf{u}}_i^n = \dot{\mathbf{u}}_i^{n-1} + \ddot{\mathbf{u}}_i^n \cdot \Delta t \tag{14}$$

$$\mathbf{u}_i^n = \mathbf{u}_i^{n-1} + \dot{\mathbf{u}}_i^n \cdot \Delta t \tag{15}$$

Although the time integration method is straightforward, the integration process is conditionally stable. Strict requirement of time intervals should be achieved for explicit algorithm. Silling and Askari (2005) applied the von Neumann stability analysis to limit the time step size Δt, which optimizes the stability of the explicit time integration

$$\Delta t < \sqrt{\frac{2\rho}{\sum V C_{ip}}} \tag{16}$$

where ρ is material density, V unit volume occupied by material point and $C_{ip} = \partial \mathbf{f} / \partial \boldsymbol{\eta}$.

4.3. Interaction force

In the case of interact problem, a force between material points belong to different bodies is defined by Madenci and Oterkus (2014). This kind of force is based on a critical distance, r_{sh}, between two material points of two different bodies when they come close to each other. Since specific two points is close enough, they begin to push each other in order to prevent sharing a same location. The force for interaction is expressed as

$$\boldsymbol{f}_{sh}(y_j, y_n) = \frac{y_j - y_n}{|y_j - y_n|} \min\left\{0, c_{sh}\left(\frac{|y_j - y_n|}{2r_{sh}} - 1\right)\right\} \tag{17}$$

where the force constant, c_{sh}, can be chosen as

$$c_{sh} = 5c \tag{18}$$

where c is called micro-modulus in bond-based peridynamics. For 3-D peridynamic simulation, c is expressed as

$$c = \frac{18k}{\pi \delta^4} \tag{19}$$

where k is bulk modulus of material.

And critical distance, r_{sh}, can be chosen as

$$r_{sh} = \frac{\Delta x}{2} \tag{20}$$

Eq. (17) was proposed in EMU manual which is a computational platform for peridynamics developed by Sandia National Laboratory. It was originally proposed for bond-based peridynamics. However, this method is able to represent good results in present simulation.

5. Numerical simulation

This section presents the process of developing a numerical simulation, including the operating conditions and numerical parameters, and the numerical results obtained from the simulation. Peridynamic simulations are implemented by Fortran codes and compiled in Intel Visual Fortran platform. Required data and visualization are plotted in Tecplot 360 software. To verify the feasibility of this numerical method, ice forces of three operating conditions with different moving velocities were compared with experimental data.

5.1. Problem setup

Numerical examples were conducted by pushing a rigid cylindrical structure through level ice with the peridynamic method. The pile diameter and length were $d = 50$ mm and $l = 500$ mm, respectively. The pile that impacts the ice sheet moves with various velocities from 30 mm/s to 1 m/s. Because the pile vibration is not considered, the pile modeled numerically by peridynamics is a rigid body that is free from deformation. Level ice is a rectangular ice sheet and its length, width and thickness as impacted by the pile are $L = 1$ m, $W = 1$ m and $T = 0.06$ m, respectively. The edges of the ice sheet, except the one interacting with the pile, are fixed. The configuration of the numerical setup is shown in Fig. 4. The material properties of the ice plate are given as an elastic modulus of $E = 120$ Mpa, mass density of $\rho = 900$ kg/m^3 and Poisson's ratio of $\nu = 0.3$.

For peridynamic method, balance of sufficient accuracy and numerical efficiency regarding with number of grid points is of great importance. According to Madenci and Oterkus (2014), grid size convergence was analyzed considering the vibration of bar. To visualize the effect of grid size on numerical error, numerical models with four grid sizes, $\Delta x = L/10, L/100, L/1000$ and $10000/L$, are developed. The results show that the error of coarse grid $\Delta x = L/10$ increases with simulation process and the other conditions meet the requirement of accuracy. Furthermore, convergence analysis involving with horizon size recommends a grid size of $\delta = 3 \cdot \Delta x$ to reduce computational time and dependence on crack propagation. In this paper, a grid spacing of 10 mm was used in the peridynamic model, which means that the ice plate includes approximately 60,000 material points. Horizon radius is $\delta = 3 \cdot \Delta x$. According to the principle of time stability, the size of the time step is 4.66×10^{-6} s. The critical equivalent strain, E_{cr}, is 0.0325. The boundary region of the ice plate contains three layers of material points on each edge which are fixed and free of deformation. In the simulation, six pile velocities were used: $v = 50$ mm/s, $v = 130$ mm/s,

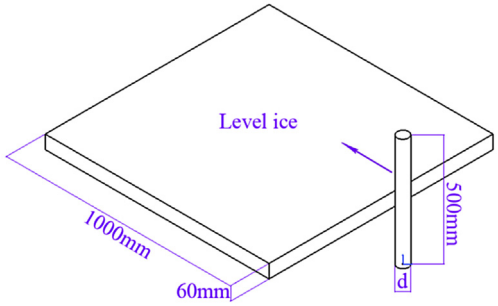

Fig. 4. Schematic diagram of interaction between level ice and cylindrical structure.

Please cite this article in press as: Liu, M., et al., Peridynamic simulation of brittle-ice crushed by a vertical structure, International Journal of Naval Architecture and Ocean Engineering (2016), http://dx.doi.org/10.1016/j.ijnaoe.2016.10.003

v = 210 mm/s, v = 500 mm/s, v = 750 mm/s and v = 1000 mm/s. Among these operating conditions, the output of the first three velocities were extracted for comparison with the experimental results.

5.2. Numerical results

Figs. 5–10 represent the total ice forces during contact of the cylindrical structure with level ice computed by peridynamics. The results are filtered using a 150-Hz low-pass filter. Similar to experimental ice-force curves obtained by Sodhi and Morris (1986), the total ice forces obtained from numerical simulation represent a typical repetitive nature and frequencies of the ice forces increase with increasing cylindrical structure velocity. In addition, each periodical involves at least two typical peaks, one with a higher value and the others with less. This phenomenon is also visible in the ice force figure with a pile velocity of 50 mm/s.

The stress state of ice sheet near the vertical structure is compression. As we know, the mechanism behavior of ice under compression is really complex. According to Yue et al. (2009), since compressive strength of ice is sensitive to strain rate, ice crushing force can be divided into three modes: 1) Ductile behavior under low strain rate. The ice in this state undergoes plastic deformation and few cracks can be observed. 2) Brittle behavior under high strain rate. Ice fails with several major cracks and little deformation can be observed. 3) Ductile-brittle transition under medium strain rate. Micro cracks form with no propagation. Compressive strength of ice varies in different states.

Table 1 shows the mean and maximum total forces during contact of the cylindrical structure with level ice. By comparing the ice forces from simulation and experiment, respectively, we can see the values of peak forces and mean forces of simulation are in the same order as experimental data. However, the peak forces from the experimental results change with cylindrical structure velocity. The reason for this problem, perhaps, is that the ductile-brittle transition is caused by different loading rates. In contrast, in this paper, ice forces obtained by peridynamics are independent of strain rate. Because only a linear elastic-brittle constitutive is used in numerical simulation. Furthermore, urea ice is used in the scale test and the influence of urea on mechanical properties is undetermined. For numerical simulation, constitutive models involved with strain rate mostly need empirical parameters, which is of difficulty to apply urea ice in simulation. The

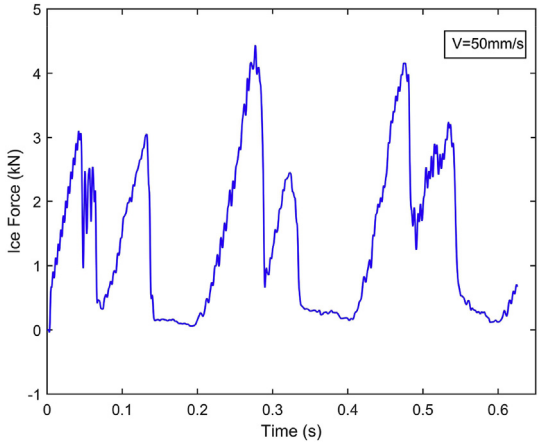

Fig. 5. Ice force from simulation (v = 50 mm/s).

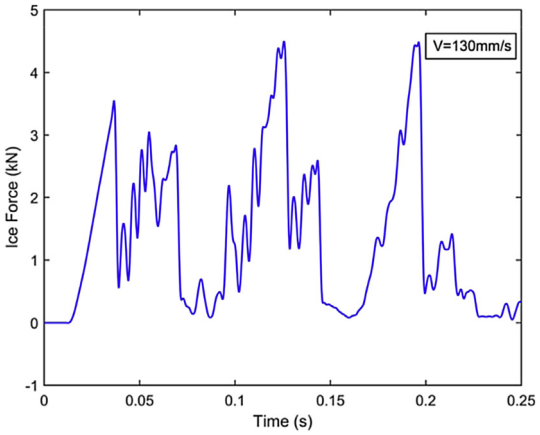

Fig. 6. Ice force from simulation (v = 130 mm/s).

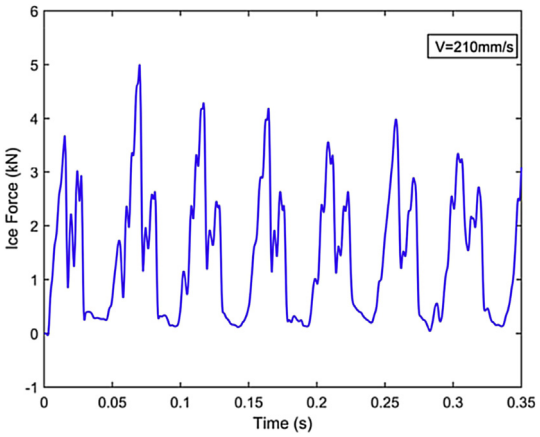

Fig. 7. Ice force from simulation (v = 210 mm/s).

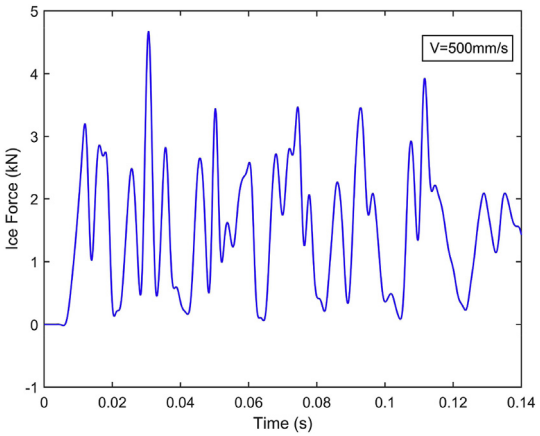

Fig. 8. Ice force from simulation (v = 500 mm/s).

Please cite this article in press as: Liu, M., et al., Peridynamic simulation of brittle-ice crushed by a vertical structure, International Journal of Naval Architecture and Ocean Engineering (2016), http://dx.doi.org/10.1016/j.ijnaoe.2016.10.003

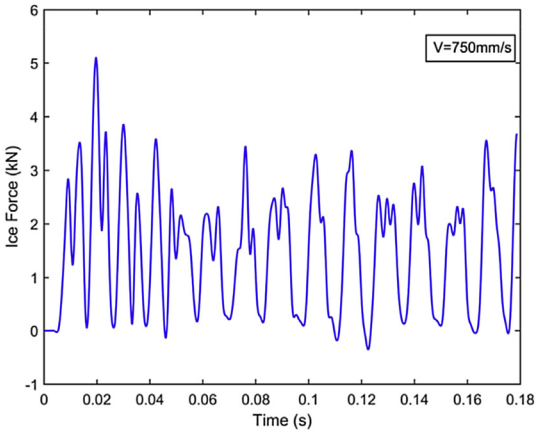

Fig. 9. Ice force from simulation (v = 750 mm/s).

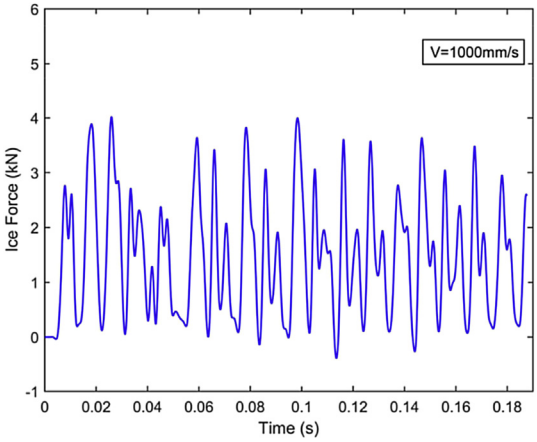

Fig. 10. Ice force from simulation (v = 1000 mm/s).

Table 1
Comparison of ice force (simulation vs. experiment).

	Velocity (mm/s)	Simulation	Experiment
Mean force (kN)	50	1.3848	5.3859
	130	1.3739	1.7309
	210	1.4324	1.9136
Peak force (kN)	50	4.4379	13.0527
	130	4.6342	5.2479
	210	4.9742	3.8522

numerical computation considering strain rate of ice will be analyzed in future research.

The results are based on a simulation with the peridynamic method and data recorded during the interaction. The simulation only shows failure of ice crushing during the interaction between the cylinder structure and the level ice. Figs. 11–14 shows peridynamic visualization of a pile moving through an ice sheet at 750 mm/s.

The simulation images show the progress of ice crushing failure, and color differences stand for the equivalent stress distribution. A high-stress field is initiated around the cylindrical structure and spreads to most areas of the ice sheet. An accumulation of damaged ice particles is visible in front of the

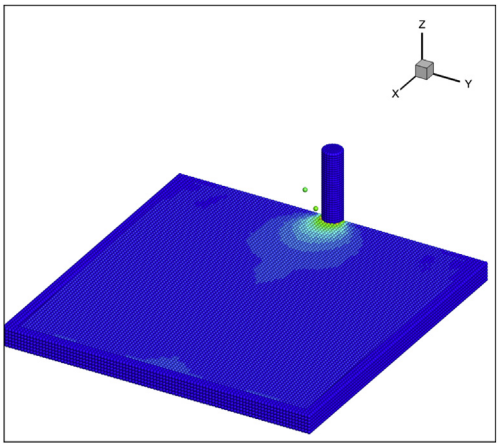

Fig. 11. Step 10,000 of simulation (v = 750 mm/s).

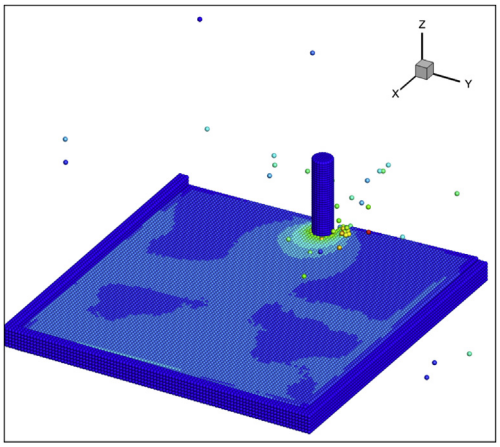

Fig. 12. Step 26,000 of simulation (v = 750 mm/s).

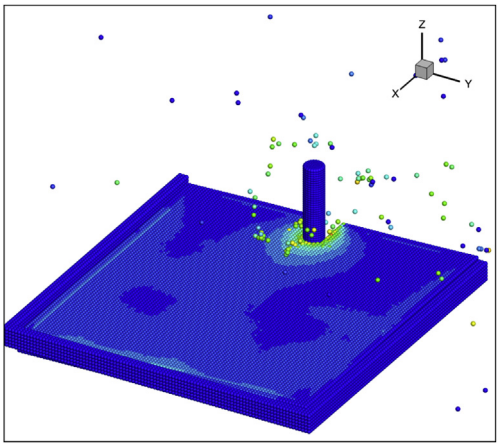

Fig. 13. Step 40,000 of simulation (v = 750 mm/s).

pile. This phenomenon is also captured by experimental record. Fig. 16 is an experimental picture of brittle ice failure induced by vertical structure crushing ice sheet. In addition, in the path cleared by cylindrical structures in peridynamic simulation, line-like hot spot can be observed, which means high stress area arranging ice thickness and occupying one

Please cite this article in press as: Liu, M., et al., Peridynamic simulation of brittle-ice crushed by a vertical structure, International Journal of Naval Architecture and Ocean Engineering (2016), http://dx.doi.org/10.1016/j.ijnaoe.2016.10.003

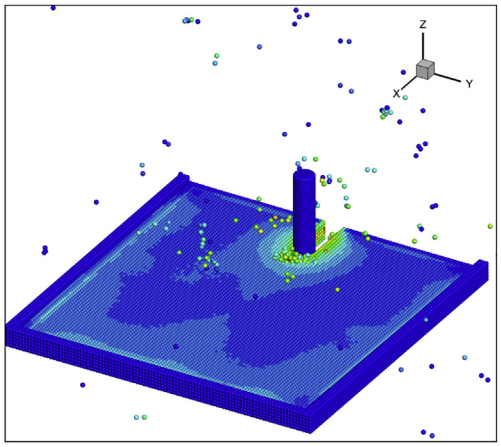

Fig. 14. Step 56,000 of simulation (v = 750 mm/s).

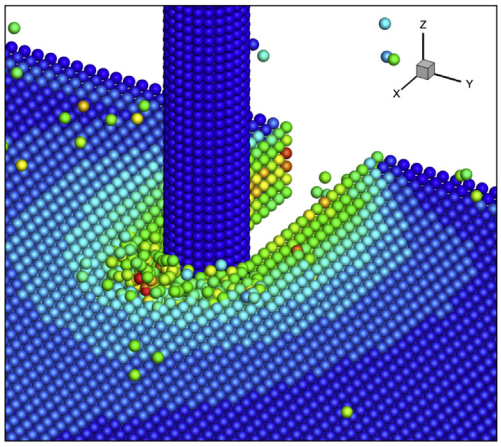

Fig. 15. Local damage in PD simulation.

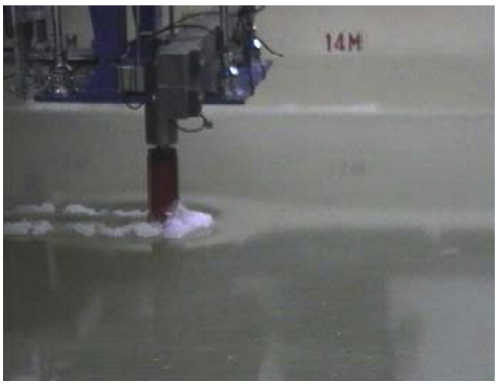

Fig. 16. Brittle ice failure of ice sheet (Huang et al., 2007).

third of total thickness. See Fig. 15. This phenomenon is caused by high level of freedom at top and below surface and be a typical phenomenon of ice crushing (Jordaan, 2001). Compared with conventional numerical techniques, such as finite element method where the failure mode is dependent on the mesh, these images show the advantages of using a meshfree method.

Morphology of ice crushing failure in peridynamic simulation matches the experimental phenomenon proposed by Sodhi and Morris (1984) and Huang et al. (2007). Simulated ice failure is mainly caused by spalling and extrusion and obvious crack involving splitting is not observed. In some experiments, large crack occasionally happened along with crushing path. This discrepancy perhaps is induced by high confinements and grid size. High confinements caused by boundary conditions may prevent the crack propagation in ice. At the same time, for peridynamics, material failure happens spontaneously and identification of specific components of failure needs more work to be achieved.

5.3. Discussion

The ice forces show secondary peak forces accompanied by true peak values, especially for the 50 mm/s velocity in experiments. Fortunately, this phenomenon was captured in the computational simulation by peridynamics.

According to Sodhi and Morris (1986), the repetitive nature of the ice forces can be characterized by determining the dominant frequency at which the ice forces vary. This is defined as the “characteristic frequency of ice failure”. To determine the characteristic frequency, force data for each velocity of pile were transformed into a frequency domain by the Fast-Fourier-Transform (FFT) routine. Figs. 17–22 show the results of the transformation. It is obvious that the frequency of ice failure increases with increasing velocity of the moving structure. In addition, variations in increasing the frequency maintain a slightly increasing trend.

During each loading cycle, the ice–structure interaction undergoes three stages: interaction, crushing and failure. At the beginning of the ice–structure interaction, the ice force appears to be increasing. Thereafter, as the pile continues to crush the ice sheet, the ice force increases with crushing distance. Finally, ice failure emerges when the crushing distance reaches a critical value. To quantify the distance the ice or structure moves for each loading cycle, a term “damage zone” was proposed by Sodhi and Morris (1986). The distance that the ice or pile moves for each loading cycle is termed as the

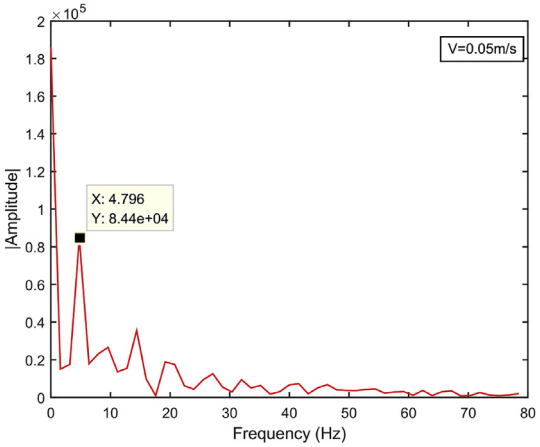

Fig. 17. FFT of ice failure (v = 50 mm/s).

Please cite this article in press as: Liu, M., et al., Peridynamic simulation of brittle-ice crushed by a vertical structure, International Journal of Naval Architecture and Ocean Engineering (2016), http://dx.doi.org/10.1016/j.ijnaoe.2016.10.003

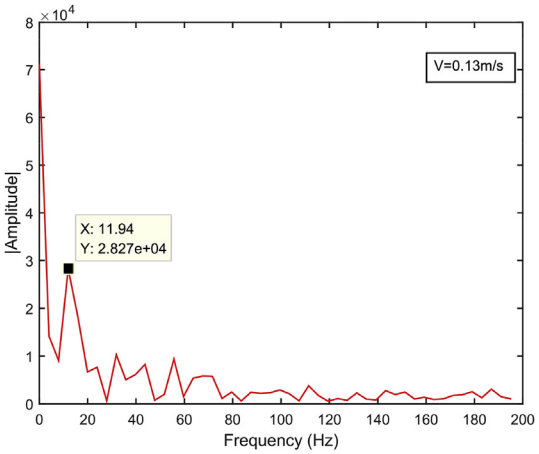

Fig. 18. FFT of ice failure (v = 130 mm/s).

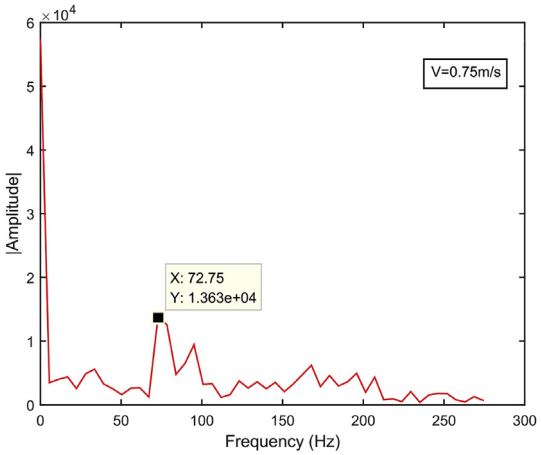

Fig. 21. FFT of ice failure (v = 750 mm/s).

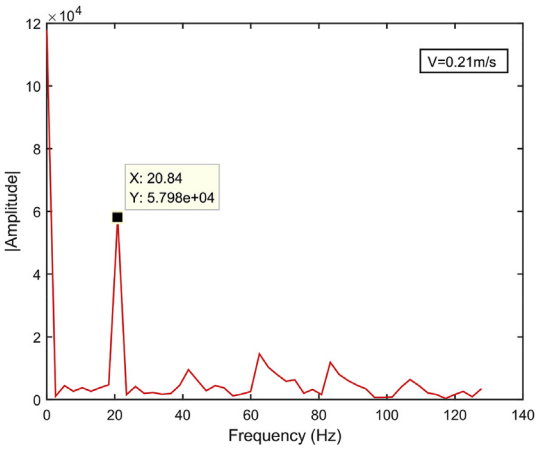

Fig. 19. FFT ice failure (v = 210 mm/s).

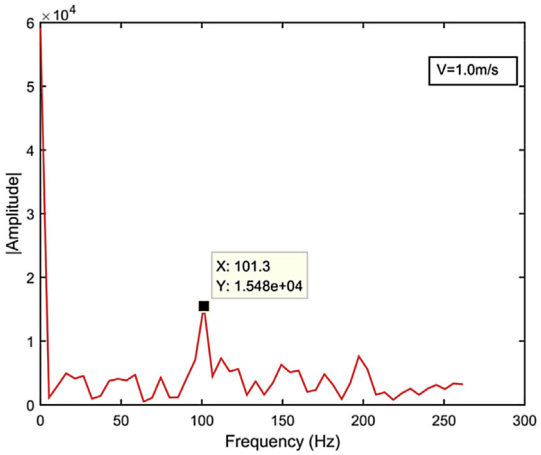

Fig. 22. FFT of ice failure (v = 1000 mm/s).

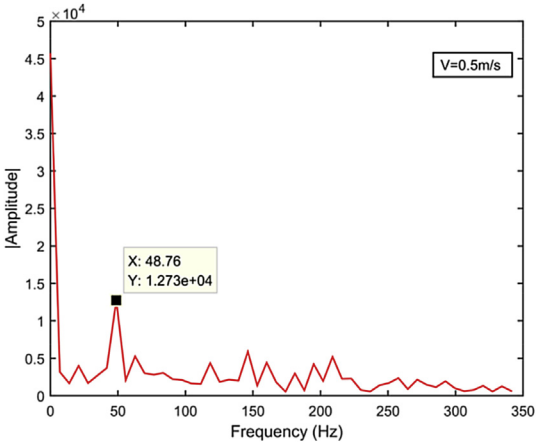

Fig. 20. FFT of ice failure (v = 500 mm/s).

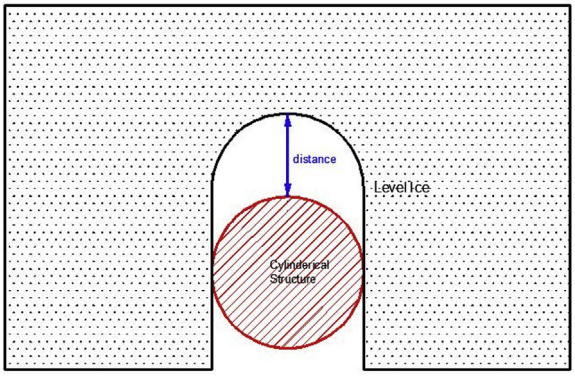

Fig. 23. Schematic diagram of characteristic ice failure.

"damage zone length", see Fig. 23. The average length δ for each loading cycle can be expressed as

$$\delta = \frac{v}{f} \tag{21}$$

where v is the pile velocity and f is the frequency of the repetitive force.

Fig. 24 shows a plot of δ/h (h is the level ice thickness) versus moving pile velocity. The damage zone length for all simulations maintained between 0.15 and 0.2 times as the ice thickness. The slightly increasing damage zone length for increasing velocities agrees well with the experimental result,

Please cite this article in press as: Liu, M., et al., Peridynamic simulation of brittle-ice crushed by a vertical structure, International Journal of Naval Architecture and Ocean Engineering (2016), http://dx.doi.org/10.1016/j.ijnaoe.2016.10.003

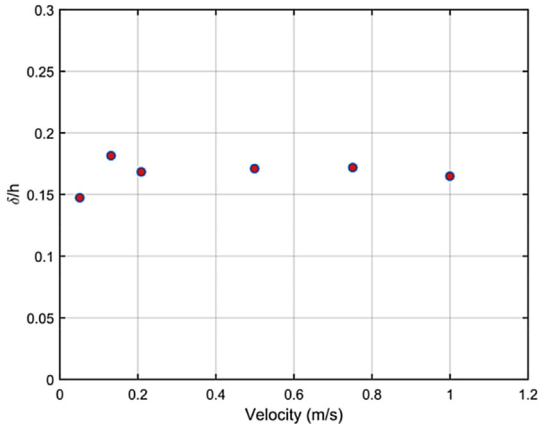

Fig. 24. Plot of δ/h (h is the thickness of level ice) versus moving pile velocities.

even though the significance of the scattered data trend is unknown.

6. Conclusions

The peridynamic model was applied to simulate the interaction of level ice and a cylindrical, vertical, rigid structure at different moving velocities. To implement two-body interactions in the peridynamic model, an interaction force density was applied to prevent the material particles that belong to different bodies from sharing the same position. To determine the feasibility and accuracy of applying the peridynamic method on ice–structure interactions, results from the peridynamic simulation were compared with small-scale experiments conducted by Sodhi and Morris. The ice force records from the numerical simulation show a typically repetitive nature and the value of the ice forces obtained by peridynamic simulation is of the same order as that of the small-scale experiments. Visual results show that during moving of the structure to crush the ice, damaged ice particles accumulate in front of the cylindrical structure, which implies the superiority of the peridynamic method to complex material damage. In addition, in the path cleared by cylindrical structures, line-like hot spot can be observed, which is high stress area arranging ice thickness and occupying one third of total thickness. A study of the characteristics of loading cycle and Fast-Fourier-Transforms were used to transform the force records from a time to a frequency domain. The characteristic ice failure frequencies increase with increasing velocities of the moving vertical structure. In addition, the lengths of the damage zones were calculated for each loading cycle. The damage zone lengths remain 0.15–0.2 times as the ice thickness. The lengths of the damage zones increase slightly with increasing moving velocities, even though the significance of this scattered data trend is unknown.

References

Bergan, P.G., Cammaert, G., Skeie, G., et al., 2010. On the potential of computational methods and numerical simulation in ice mechanics[C]//. IOP Conf. Ser. Mater. Sci. Eng. 10 (1), 012102. IOP Publishing.

Brbaru, F., Yang, M., Alves, L.F., Silling, S.A., Askari, E., Xu, J., 2009. Convergence, adaptive refinement, and scaling in 1D peridynamic. Int. J. Numer. Methods Eng. 77 (6), 852–877.

Foster, J.T., Silling, S.A., Chen, W.W., 2010. Viscoplasticity using peridynamics. Int. J. Numer. Methods Eng. 81 (10), 1242–1258.

Huang, Y., Shi, Q., Song, A., 2007. Model test study of the interaction between ice and a compliant vertical narrow structure. Cold Reg. Sci. Technol. 49 (2), 151–160.

Jones, S.J., 1982. The confined compressive strength of polycrystalline ice. J. Glaciol. 28, 171–177.

Jordaan, I., 2001. J. Mechanics of ice–structure interaction. Eng. Fract. Mech. 68 (17), 1923–1960.

Kamio, Z., Matsushita, H., Strnadel, B., 2003. Statistical analysis of ice fracture characteristics. Eng. Fract. Mech. 70 (15), 2075–2088.

Kuehn, G.A., Schulson, E.M., Jones, D.E., et al., 1993. The compressive strength of ice cubes of different sizes. J. Offshore Mech. Arct. Eng. 115 (2), 142–148.

Madenci, E., Oterkus, E., 2014. Peridynamic Theory and its Applications. Springer, New York.

Schulson, E.M., 2001. Brittle failure of ice. Eng. Fract. Mech. 68 (17), 1839–1887.

Schulson, E.M., 1997. The brittle failure of ice under compression. J. Phys. Chem. B 101 (32), 6254–6258.

Silling, S.A., 2000. Reformulation of elasticity theory for discontinuities and long-range forces. J. Mech. Phys. Solids 48 (1), 175–209.

Silling, S.A., Askari, E., 2005. A meshfree method based on the peridynamic model of solid mechanics. Comput. Struct. 83 (17), 1526–1535.

Silling, S.A., Epton, M., Weckner, O., et al., 2007. Peridynamic states and constitutive modeling. J. Elast. 88 (2), 151–184.

Sodhi, D.S., Morris, C.E., 1984. Ice Forces on Rigid, Vertical, Cylindrical Structures. Cold Regions Research and Engineering Lab, Hanover NH.

Sodhi, D.S., Morris, C.E., 1986. Characteristic frequency of force variations in continuous crushing of sheet ice against rigid cylindrical structures. Cold Reg. Sci. Technol. 12 (1), 1–12.

Warren, T.L., Silling, S.A., Askari, A., et al., 2009. A non-ordinary state-based peridynamic method to model solid material deformation and fracture. Int. J. Solids Struct. 46 (5), 1186–1195.

Tian,, Y., Yan, H., 2013. The dynamic ice loads on conical structures. Ocean Eng 59, 37–46.

Yue, Q., Guo, F., Kärnä, T., 2009. Dynamic ice forces of slender vertical structures due to ice crushing. Cold Reg. Sci. Technol. 56 (2–3), 77–83.

Please cite this article in press as: Liu, M., et al., Peridynamic simulation of brittle-ice crushed by a vertical structure, International Journal of Naval Architecture and Ocean Engineering (2016), http://dx.doi.org/10.1016/j.ijnaoe.2016.10.003